

## Elastic and anelastic relaxations associated with phase transitions in $\text{EuTiO}_3$

Leszek J. Spalek

*Cavendish Laboratory, University of Cambridge, Madingley Road, Cambridge CB3 0HE,  
United Kingdom and Faculty of Physics and Applied Computer Science, AGH University of  
Science and Technology, al. Mickiewicza 30, 30-059 Krakow, Poland*

Siddharth S. Saxena

*Cavendish Laboratory, University of Cambridge, Madingley Road, Cambridge CB3 0HE,  
United Kingdom*

Christos Panagopoulos

*Division of Physics and Applied Physics, Nanyang Technological University, 637371  
Singapore, Singapore and Department of Physics, University of Crete and FORTH, GR-  
71003 Heraklion, Greece*

Takuro Katsufuji

*Department of Physics, Waseda University, Tokyo 169-8555, Japan*

Jason A. Schiemer and Michael A. Carpenter

*Department of Earth Sciences, University of Cambridge, Downing Street, Cambridge CB2  
3EQ, United Kingdom*

PACs numbers: 62.20.de, 62.40.+i, 64.60.Ej, 75.85.+t

### Abstract

Elastic and anelastic properties of single crystal samples of  $\text{EuTiO}_3$  have been measured between 10 and 300 K by Resonant Ultrasound Spectroscopy at frequencies in the vicinity of 1 MHz. Softening of the shear elastic constants  $C_{44}$  and  $\frac{1}{2}(C_{11} - C_{12})$  by ~20-30% occurs with

falling temperature in a narrow interval through the transition point,  $T_c = 284$  K, for the cubic - tetragonal transition. This is accounted for by classical coupling of macroscopic spontaneous strains with the tilt order parameter, in the same manner as occurs in  $\text{SrTiO}_3$ . A peak in the acoustic loss occurs a few degrees below  $T_c$  and is interpreted in terms of initially mobile ferroelastic twin walls which rapidly become pinned with further lowering of temperature. This contrasts with the properties of twin walls in  $\text{SrTiO}_3$  which remain mobile down to at least 15 K. No further anomalies were observed that might be indicative of strain coupling to any additional phase transitions above 10 K. A slight anomaly in the shear elastic constants, independent of frequency and without any associated acoustic loss, was found at  $\sim 140$  K. It marks a change from elastic stiffening to softening with falling temperature and perhaps provides evidence for coupling between strain and local fluctuations of dipoles related to the incipient ferroelectric transition. An increase in acoustic loss below  $\sim 80$  K is attributed to the development of dynamical magnetic clustering ahead of the known antiferromagnetic ordering transition at  $\sim 5.5$  K. Detection of these elastic anomalies serves to emphasise that coupling of strain with tilting, ferroelectric and magnetic order parameters is likely to be a permeating influence in determining the structure, stability, properties and behaviour of  $\text{EuTiO}_3$ .

## I. INTRODUCTION

The perovskite  $\text{SrTiO}_3$  has been investigated intensively over many years with regard to its antiferrodistortive structural phase transition and quantum paraelectricity,<sup>1,2</sup> not to mention the variety of subtle variations in physical properties of the tetragonal structure and of twin walls within it.<sup>3-12</sup> Substituting europium for strontium yields an isostructural system,  $\text{EuTiO}_3$ , which exhibits closely analogous structural behaviour but with the addition of antiferromagnetism below  $\sim 5.5$  K.<sup>13-29</sup> Furthermore, there is magnetoelectric coupling at low

temperatures,<sup>14,18,30,31</sup> the paramagnetic susceptibility changes through the structural transition point,  $T_c \sim 285$  K,<sup>27</sup> and  $T_c$  itself shifts by a few degrees in an externally applied magnetic field.<sup>32</sup> It is thus clear that there is coupling between magnetic and structural properties, and hence that  $\text{EuTiO}_3$  has the potential to combine ferro/antiferromagnetism, ferroelectricity and ferroelasticity. As with multiferroic materials in general, a key property relating to individual instabilities and coupling between them is strain, and it is already clear from that imposition of an external strain could lead to a particularly rich phase diagram topology.<sup>33-35</sup> This aspect of the intrinsic behaviour of  $\text{EuTiO}_3$  remains controversial, however, and has not yet been fully characterised for bulk samples.

A macroscopic tetragonal strain similar to that due to the cubic - tetragonal transition in  $\text{SrTiO}_3$  has been reported to occur below  $\sim 235$  K<sup>22</sup> or below  $\sim 285$  K.<sup>23</sup> If there is any strain coupling with the order parameter, it will inevitably give rise to relaxations of elastic properties and an anomaly has been found in the Young's modulus below 308 K, as measured by dynamical mechanical analysis at 1 Hz.<sup>23</sup> Bessas et al.<sup>26</sup> reported softening of the shear wave velocity below  $\sim 320$  K extracted from measurements made by Resonant Ultrasound Spectroscopy (RUS), but with a form that is different from the softening known to occur in  $\text{SrTiO}_3$  and summarised in Ref. 36. The primary objective of the present study was to resolve these discrepancies and address the question of strain relaxation associated with the structural transition by measuring elastic and anelastic properties in the temperature interval 10-300 K. We report 20-30 % softening of single crystal elastic constants between  $\sim 290$  and  $\sim 280$  K which is larger than, though closely analogous with what is found in association with the octahedral tilting transition in  $\text{SrTiO}_3$ . The pattern of anelastic loss is quite different from that seen in  $\text{SrTiO}_3$ , however, which brings into focus the nature and properties of ferroelastic twin walls of  $\text{EuTiO}_3$ . There are other minor anomalies in elastic/anelastic behaviour at lower temperatures but these are substantially smaller than the relaxational effects which are

associated with  $T_c$ .

If the analogy with  $\text{SrTiO}_3$  is correct, the expectation is that the driving mechanism for the structural transition in  $\text{EuTiO}_3$  is an R-point soft optic mode to give the symmetry change  $Pm\bar{3}m \leftrightarrow I4/mcm$ . Diffraction evidence is consistent with this space group assignment for the low temperature structure,<sup>21-23</sup> and inelastic x-ray scattering results are consistent with the operation of the soft mode.<sup>17</sup> A small anomaly in the heat capacity indicates  $T_c = 282 \pm 1$  K, with a form that is similar to the anomaly associated with the transition in  $\text{SrTiO}_3$ .<sup>15,24,32</sup> This, in turn, is consistent with second order or close to second order character for the transition, as is the linear temperature dependence of the intensity of superlattice reflections observed by Ellis et al.<sup>37</sup> Variations of the lattice parameters reported by Goian et al.<sup>23</sup> and Allieta et al.<sup>22</sup> are similar in form to those shown by  $\text{SrTiO}_3$ , while a change in linear thermal expansion through the transition point is again consistent with a second order transition.<sup>23</sup> Not all samples behave in the same way, however.

In contrast with studies which report  $T_c$  for  $\text{EuTiO}_3$  as being near 285 K<sup>15,17,20,23,24,27,32,38</sup>, Bessas et al.<sup>26</sup> found no evidence for any distortion from cubic lattice geometry or of a heat capacity anomaly, and the only evidence for structural changes near 285 K was elastic softening. Kim et al.<sup>25</sup> found diffraction evidence for an incommensurate structure between  $\sim 2$  and  $\sim 285$  K, and coexistence of commensurate and incommensurate reflections between  $\sim 2$  and  $\sim 160$  K. Electron diffraction from a selected grain taken from a ground up single crystal has also revealed the presence of incommensurate reflections at room temperature, but these were no longer present when the sample was re-examined two weeks later.<sup>23</sup> Allieta et al.<sup>22</sup> found that symmetry breaking lattice distortions could be detected in a powder sample only below 235 K, even though the parent material showed the same form of heat capacity anomaly as originally reported by Bussmann-Holder et al.<sup>15</sup>. Following Bussman-Holder et al.<sup>15</sup> (their Figure 2) Bettis et al.<sup>16</sup> have argued that the free energy

potential governing the soft mode is narrow and deep, relative to  $\text{SrTiO}_3$ , and hence that the structural transition is more nearly order/disorder than displacive in character. Perhaps there are also additional effects of local disorder in  $\text{EuTiO}_3$ ,<sup>22</sup> but at least some differences between samples could arise from the sample preparation, such as defect content or stoichiometry.

## II. SAMPLE DESCRIPTION AND EXPERIMENTAL METHODS

The single crystals of  $\text{EuTiO}_3$  used for the present study came from the same two batches of crystals as those used by Allieta et al.<sup>22</sup> and Petrovic et al.<sup>24</sup> They had been grown by the floating-zone method in the laboratory of T. Katsufuji, as described in detail in Ref. 13. This method involves melting a pressed rod of  $\text{Eu}_2\text{O}_3$ , Ti and  $\text{TiO}_2$ , i.e. mixed starting materials, under an argon atmosphere inside a floating-zone furnace. An  $\text{Eu}^{2+}$  compound may be obtained despite the starting  $\text{Eu}^{3+}$  valency of  $\text{Eu}_2\text{O}_3$ , owing to an Eu to Ti charge transfer. The resulting samples are opaque (black and lustreless) at room temperature. Diffraction characteristics have been described elsewhere<sup>22,29</sup> and the level of impurities was established to be below 1%, consisting of  $\text{Eu}_2\text{Ti}_2\text{O}_7$  which is non-magnetic. A clear maximum in the heat capacity has been reported to be at 284 K<sup>29</sup> or 283 K.<sup>24</sup>, with an estimate experimental uncertainty of  $\pm 2$  K. Here 284 K is taken to be  $T_c$  for the cubic - tetragonal structural phase transition.

For RUS, a sample is held lightly between a pair of piezoelectric transducers, one of which is driven at a constant amplitude across a range of frequencies. At particular frequencies the sample resonates and the enhanced amplitudes of these normal modes are detected by the second transducer.<sup>39</sup> In the low temperature instrument at the University of Cambridge,<sup>40</sup> the sample is held inside an “Orange” helium flow cryostat with an atmosphere of a few mbars of helium gas to allow thermal equilibration. Temperature is measured with a silicon diode and is believed to represent the sample temperature to  $\pm \sim 0.1$  K. The two

crystals of  $\text{EuTiO}_3$  used had irregular shapes, with edge dimensions between  $\sim 0.5$  and  $\sim 1$  mm and masses 0.0568 gm (crystal 1), 0.0222 gm (crystal 2). For crystal 1, spectra were collected in the frequency range 0.3 – 2 MHz in 30 K steps during cooling down to 10 K followed by 5 K steps up to  $\sim 310$  K. For crystal 2, spectra were collected in the frequency range 0.1-3.0 MHz in 30K steps, all with  $\sim 15$  minutes for thermal equilibration at each temperature. The heating sequence was 5 K steps from 10 to 270 K, 1 K steps between and 270 and 290 K, followed by 5 K steps up to  $\sim 310$  K, and with 10 minutes for thermal equilibration at each temperature. Each spectrum contained 50,000 data points.

Raw spectra were analysed with the software package Igor Pro (Wavemetrics). Frequencies,  $f$ , and widths at half maximum height,  $\Delta f$ , were determined for selected peaks by fitting with an asymmetric Lorentzian function.  $f^2$  scales with the elastic constant or combination of elastic constants that determines a given resonance mode, and the inverse mechanical quality factor,  $Q^{-1} = \Delta f/f$ , is a measure of acoustic loss. The single crystals used were not regular parallelepipeds, so absolute values of the single crystal elastic constants were not determined. Interest, however, was focussed on changes in elastic and anelastic properties with temperature and, as discussed below, it proved possible to discriminate between variations of  $C_{44}$  and  $\frac{1}{2}(C_{11} - C_{12})$ .

### III. RESULTS

Figure 1 shows a segment of selected RUS spectra collected during heating of crystal 2. Each spectrum has been shifted up the y-axis (amplitude) in proportion to the temperature at which it was collected and the axis labelled as temperature. The most obvious feature is a minimum in the frequencies of most resonance peaks at  $\sim 280$  K, but there is also a change in trend at  $\sim 140$  K and softening below  $\sim 80$  K. The high temperature structure is cubic and if there are equal proportions of all possible tetragonal twins in the low temperature structure,

that too will be effectively cubic with respect to its gross elastic properties. The resonance frequencies will depend on three elastic constants which, in symmetry-adapted form, are  $\frac{1}{3}(C_{11} + 2C_{12})$ , “ $\frac{1}{2}(C_{11} - C_{12})$ ” and “ $C_{44}$ ”. Inverted commas are added to emphasise that these are effective averages for a twinned tetragonal crystal. Most resonances are determined predominantly by shearing motions and their frequencies will depend on combinations of the two shear elastic constants “ $\frac{1}{2}(C_{11} - C_{12})$ ” and “ $C_{44}$ ”. Some of the modes will be determined predominantly by “ $\frac{1}{2}(C_{11} - C_{12})$ ” and some predominantly by “ $C_{44}$ ”, but most will depend on a mixture of the two. The contribution of  $\frac{1}{3}(C_{11} + 2C_{12})$  will depend on whether the resonance mode involves some component of breathing motion but experience has shown that this tends to be small in all but a few resonances. It is possible to pick out peaks which are representative of the two limiting cases of shear motion by inspection, such as those labelled 1 and 2 in the stack of spectra in Figure 1. Peak 1 shows a marked stiffening as the transition point is approached from below while peak 2 show marked softening

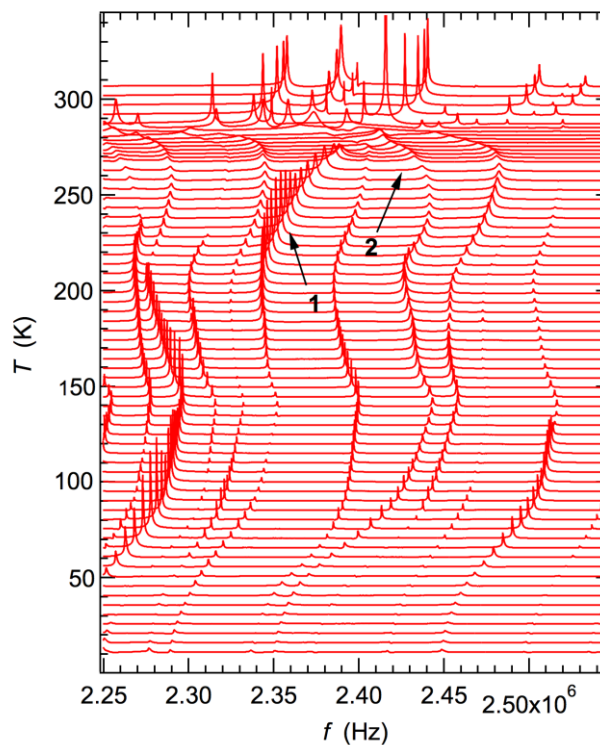


Figure 1. Segments of a selection of RUS spectra collected during heating of crystal 2. The y-axis should really be amplitude in volts, from the detector transducer, but each spectrum has been offset in proportion to the temperature at which it was collected and the axis labelled as temperature. There is an obvious steep minimum in resonance frequencies near 280 K but additional anomalies are also evident as changes in trend at  $\sim 140$  K and  $\sim 80$  K. Two trends for the temperature dependence below  $\sim 280$  K have been picked out and the relevant peaks are labelled 1 and 2. Peak 1 has stiffening as  $T \rightarrow 280$  K from below and peak 2 shows softening. The trends of all other peaks in the spectra can be represented as showing some combination of the trends of these two.

Figure 2 shows the results from fitting of resonance peaks with frequencies in the vicinity of 1 MHz at room temperature, which were selected not only as being representative of the limiting cases for the temperature evolution below  $\sim 280$  K but which could also be followed through the transition point. Experimental uncertainties in the determination of  $f^2$  are smaller than the size of the symbols. Some indication of the experimental uncertainty in absolute values of  $Q^{-1}$  derived from the fitting process is given by scatter in the data, particularly at the lowest temperatures where the resonance peaks were weak. By analogy with the observed variations of single crystal elastic constants through the same transition in  $\text{SrTiO}_3$ ,<sup>36</sup> the resonances are tentatively ascribed to “ $C_{44}$ ” (Fig. 2a) and “ $\frac{1}{2}(C_{11} - C_{12})$ ” (Fig. 2b), respectively.  $C_{44}$  for  $\text{SrTiO}_3$  shows slight increasing stiffness as  $T \rightarrow T_c$  from below while  $\frac{1}{2}(C_{11} - C_{13})$  softens very slightly. Also as in  $\text{SrTiO}_3$ , both show some softening as  $T \rightarrow T_c$  from above.  $f^2$  data representative of “ $\frac{1}{2}(C_{11} - C_{12})$ ” show softening by  $\sim 25\%$  through  $T_c$  and have a sharp minimum at  $\sim 280$  K. The equivalent softening for “ $C_{44}$ ” is  $\sim 30\%$ . This is accompanied by a steep increase in  $Q^{-1}$  in both cases, rising to a maximum value of  $\sim 0.011$  at  $\sim 279$  K for “ $\frac{1}{2}(C_{11} - C_{12})$ ”.  $Q^{-1}$  then tails down to values near 0.001, which are the same as for  $T > T_c$ , by  $\sim 220$  K.



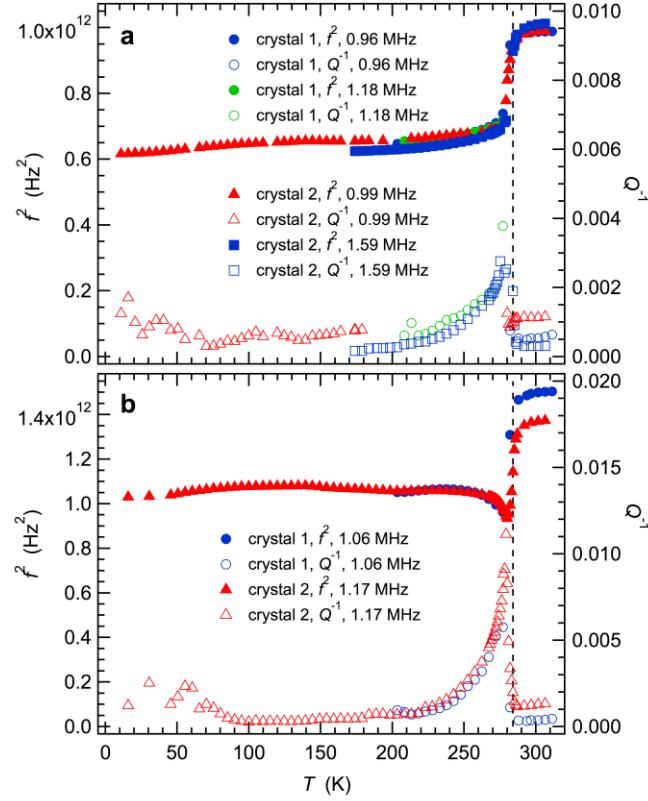


Figure 2. Variations of  $f^2$  and  $Q^{-1}$  obtained from fitting of selected resonance peaks in RUS spectra collected from both single crystals. Values of the single crystal elastic constants which determine each resonance mode scale with  $f^2$ . None of the resonances is a pure mode, in the sense of being determined by only one or two elastic constants, but the pattern shown by resonance frequencies in (a) is likely to be a good approximation for the variation of “ $C_{44}$ ” for a tetragonal crystal containing multiple ferroelastic twins. The pattern of resonance frequencies in (b) is believed to be a reasonable approximation for “ $\frac{1}{2}(C_{11} - C_{12})$ ”. Note that  $f^2$  values for different resonances have been scaled to produce close overlap below  $T_c$ ; values of their actual resonance frequencies at room temperature are given in the captions. The dashed vertical line is at 284 K.

Variations of  $f^2$  below 280 K are much smaller than those which accompany the phase transition. The change in slope at  $\sim 140$  K evident in the raw spectra (Fig. 1) is not accompanied by any overt change in  $Q^{-1}$ . On the other hand, the softening below  $\sim 80$  K is accompanied by increasing acoustic loss with falling temperature.

#### IV. DISCUSSION

The typical elastic softening associated with structural phase transitions occurs as a

consequence of classical strain/order parameter coupling and is well understood. Most or all of the elastic constants of the low symmetry phase are softer than those of the high symmetry phase and their evolution with temperature depends on the strength of coupling, the evolution of the order parameter and the evolution of the order parameter susceptibility. Expressions for these are given for the symmetry change  $Pm\bar{3}m \leftrightarrow I4/mcm$  in Ref. 36. The difference between “ $\frac{1}{2}(C_{11} - C_{12})$ ” and “ $C_{44}$ ” arises essentially because the symmetry-breaking tetragonal shear strain is  $e_t \approx (2/\sqrt{3})(c - a)/(a^2c)^{1/3}$ , where  $a$  and  $c$  are lattice parameters of the tetragonal structure while the other possible shear strain,  $e_4 \approx \cos\alpha$ , where  $\alpha$  is the rhombohedral lattice angle defined with respect to a pseudocubic reference cell) remains strictly zero. For a classical improper ferroelastic transition that is second order in character, the softening is expected to be a step at  $T = T_c$  by an amount that is independent of temperature. The slightly upward curve of “ $C_{44}$ ” as  $T \rightarrow T_c$  from below arises as a consequence of the contribution from sixth order terms in the Landau free energy and becomes steeper as the character of the transition changes from second order towards tricritical. Non-linear softening of “ $\frac{1}{2}(C_{11} - C_{12})$ ” as  $T \rightarrow T_c$  from below also arises from the contribution of sixth order terms. The overall pattern in Figure 2 is thus consistent with a second order transition that could be well represented by a Landau 246 potential, as for  $\text{SrTiO}_3$ . Superimposed on the classical picture is softening as  $T \rightarrow T_c$  from above due to fluctuations. This is again typical of octahedral tilting transitions in perovskites, such as  $\text{SrTiO}_3$ ,<sup>36</sup>  $\text{SrZrO}_3$ ,<sup>41</sup>  $\text{LaAlO}_3$ <sup>42</sup> and  $\text{KMnF}_3$ ,<sup>43</sup> for example. The elastic constants do not by themselves give a precise transition temperature, but there are no gross features in the resonance frequencies which would indicate phase transitions at any temperature other than that indicated by the heat capacity anomaly as occurring at  $T_c = 284$  K.

The total softening of “ $\frac{1}{2}(C_{11} - C_{12})$ ” in  $\text{EuTiO}_3$ , representing an average of combinations of  $C_{11}$ ,  $C_{33}$ ,  $C_{12}$  and  $C_{13}$ , is  $\sim 25\%$  and the total softening of “ $C_{44}$ ” (average of  $C_{44}$ ,  $C_{66}$ ) is  $\sim 30\%$ . Both are larger than observed for  $\text{SrTiO}_3$ , which, based on the data in Ref. 36 would be  $\sim 10\text{-}15\%$  and  $\sim 15\text{-}20\%$  respectively. The amount of softening of “ $\frac{1}{2}(C_{11} - C_{12})$ ” due to coupling of  $e_t$  with the driving order parameter is expected to scale with  $\lambda^2/b_L$  for a second order phase transition, where  $\lambda$  is the coupling coefficient and  $b_L$  the (unrenormalised) fourth order Landau coefficient. Some semiquantitative comparison of these parameters can be made to show whether there are gross differences in thermodynamic properties for the two materials.  $e_t$  is expected to scale with the octahedral tilt angle,  $\phi$ , according to  $e_t \mu / f^2 / (C_{11}^o - C_{12}^o)$ , where  $(C_{11}^o - C_{12}^o)$  is a shear elastic constant of the parent cubic structure. Taking values of the lattice parameters,  $a \approx 3.898$  and  $c \approx 3.906$  Å at 170 K ( $T/T_c = 0.6$ ) from Figure 1 of Goian et al.<sup>23</sup> gives  $e_t \approx 0.0024$ . From the same figure, the tilt angle is  $\sim 3.6^\circ$ , giving  $e_t / f^2 \sim 0.00019$ . In the case of  $\text{SrTiO}_3$ , strains from Ref. 36 and tilt angles from Ref. 44 give  $e_t / f^2 \sim 0.00021$  at  $T/T_c = 0.6$  ( $e_t \sim 0.0006$ ,  $\phi \sim 1.7^\circ$ ). It appears, therefore, that the relationship between shear strain and tilt angle is about the same. However, absolute values of  $e_t$  are a factor of  $\sim 4$  greater for  $\text{EuTiO}_3$  than for  $\text{SrTiO}_3$  and magnitudes of the coupling coefficient depend on the value of the strain with respect to the order parameter,  $q$ , which would be the same for a given value of  $T/T_c$ . Thus,  $\lambda$  for coupling between  $q$  and  $e_t$  will be a factor of  $\sim 4$  greater for  $\text{EuTiO}_3$  and  $\lambda^2$  a factor of  $\sim 16$  greater. Estimates of other thermodynamic parameters can be obtained from heat capacity data. The excess heat capacity,  $\Delta C_p$ , at  $T = T_c$  is  $1.5 \pm 0.35$  J.mole<sup>-1</sup>.K<sup>-1</sup> in Figure 2 of Petrovic et al.<sup>24</sup>, which gives a value for the Landau  $a$  coefficient,  $a_L$ , of  $3.0 \pm 0.7$  J.mole<sup>-1</sup>.K<sup>-1</sup>, assuming second order character for the transition ( $\Delta C_p = aT/2T_c$ ). This compares with  $0.65$  J.mole<sup>-1</sup>.K<sup>-1</sup> determined for  $\text{SrTiO}_3$  by

Hayward and Salje.<sup>45</sup> Assuming second order character again would give  $b_L^* = aT_c = 852 \pm 199 \text{ J.mole}^{-1}$  for  $\text{EuTiO}_3$ , where  $b^*$  is the fourth order Landau coefficient, including renormalisation by coupling with strains. On the same basis,  $b_L^*$  for  $\text{SrTiO}_3$  would be  $\sim 69 \text{ J.mole}^{-1}$ , which is a factor of  $\sim 12 \pm 3$  smaller than for  $\text{EuTiO}_3$ . Ignoring the difference between  $b_L^*$  and  $b_L$  due to strain renormalisation, softening of “ $\frac{1}{2}(C_{11} - C_{12})$ ” scaled as  $\lambda^2/b_L$  would be a factor  $\sim 16/(12 \pm 3)$ , i.e. 1.1 – 1.8, greater for  $\text{EuTiO}_3$  than for  $\text{SrTiO}_3$ . This is sufficiently close to the observed factor of  $\sim 2$ , for it to be at least concluded that strain and elastic relaxations at the  $Pm\bar{3}m \leftrightarrow I4/mcm$  transition are probably rather similar for  $\text{SrTiO}_3$  and  $\text{EuTiO}_3$ .

Accompanying the acoustic loss observed immediately below  $T_c$  must be some anelastic softening, slightly enhancing the steepness of the dip in “ $\frac{1}{2}(C_{11} - C_{12})$ ” according to standard Debye relations, in comparison with what would occur as a consequence of the strain/order parameter coupling alone. It is most likely due to the mobility under stress of ferroelastic twin walls but, in this regard, the pattern of behaviour appears to be very different from that of  $\text{SrTiO}_3$ . A remarkable feature of tetragonal  $\text{SrTiO}_3$  is high mobility of twin walls down to at least  $\sim 15 \text{ K}$  at both  $\text{Hz}^{7-9}$  and  $\text{MHz}^{12,46}$  frequencies. By way of contrast, the peak in  $Q^{-1}$  immediately below  $T_c$  in  $\text{EuTiO}_3$  (Fig. 2) occurs in a narrow temperature interval, implying that the twin walls quickly become immobile with falling temperature. A better analogy is probably provided by the  $Pm\bar{3}m \leftrightarrow R\bar{3}c$  octahedral tilting transition in  $\text{LaAlO}_3$  at  $817 \text{ K}$ .<sup>47-49</sup> When measured at frequencies of  $\sim 1\text{-}100 \text{ Hz}$  by dynamical mechanical analysis there is a temperature interval of  $\sim 250 \text{ K}$  below  $T_c$  in which there is a plateau in the loss due to twin wall motion modified by an effective viscous drag. The freezing interval where the walls become pinned by the defects is then marked by a Debye loss peak near  $450 \text{ K}$ . Under the higher frequency ( $\sim 1 \text{ MHz}$ ) and relatively low stress conditions of an RUS experiment,

acoustic losses are sufficiently high that details of the plateau region are not seen because resonance peaks are totally attenuated (superattenuation). The pinning process is still complete by  $\sim 400$  K, however.<sup>42</sup> If the twin walls in  $\text{EuTiO}_3$  are subject to pinning by oxygen vacancies as in  $\text{LaAlO}_3$ , it is likely that their freezing interval will also be in the vicinity of  $\sim 450$  K, ie well above  $T_c$ . In this case the observed variations in  $Q^{-1}$  most likely reflect changes in the number density,  $N$ , and thickness,  $w$ , of ferroelastic twin walls which are expected to increase according to  $w \propto N \propto (T_c - T)^{-1}$  as  $T \rightarrow T_c$ .<sup>50-53</sup> Interaction of the twin walls with the underlying lattice and point defects is known to be stronger for thin walls than thick walls.<sup>54,55</sup> As a consequence, the low density of thick walls expected to appear immediately below  $T_c$  at a second order transition would be expected to cause only limited attenuation. As their number goes up and their thickness goes down, there should be a steep increase in acoustic loss, until they become sufficiently thin that they become pinned. With further falling temperature, the acoustic loss will fall off steeply, therefore. In detail the actual loss mechanism at RUS frequencies is most likely due to lateral motion of ledges within the walls.<sup>43,56,57</sup>

With further lowering of temperature there are additional anomalies in the data for  $f^2$  and  $Q^{-1}$  which, although small in comparison with the softening at  $T_c$ , must be indicative of additional relaxational effects. From diffraction evidence, Ellis et al.<sup>17</sup> detected the development of obvious twinning below  $\sim 250$  K in a single crystal in which the intensity of an R-point reflection went to zero at  $T_c = 287 \pm 1$  K.  $Q^{-1}$  reduces to baseline levels in the vicinity of  $\sim 220$  K (Fig. 2), but there are no obvious breaks in trend which would signify abrupt changes in the configuration or properties of the twin walls. It is likely that they become more readily distinguishable by X-ray diffraction when they also become thinner and less mobile. 235 K is also the temperature at which the diffraction data in Allieta et al.<sup>22</sup> from a powdered sample show the tetragonal strain going to zero, but there is no evidence for this

in the temperature dependence of  $f^2$  from a single crystal.

There is a clear break in slope of resonance frequencies at  $\sim 140$  K. This is most obvious in the raw spectra (Fig. 1) and marks a change in trend from stiffening to softening with falling temperature. An anelastic origin can be ruled out because the anomaly in  $f^2$  occurs at the same temperature across the entire frequency range in which resonance peaks were observed,  $\sim 0.8$ - $2.6$  MHz, and is not accompanied by any obvious changes in  $Q^{-1}$ . The only reported structural change is a crossover from a structural state with both R-point and incommensurate superstructure reflections in single crystal X-ray diffraction patterns, below  $\sim 160$  K, to one with incommensurate reflections only, above  $\sim 160$  K,<sup>25</sup> but the single crystal used in the present study has not been characterised in the same way. The other possibility relates to the incipient ferroelectric transition. The soft mode for this reduces in frequency with falling temperature from at least 600 K and would give an extrapolated transition point near  $-200$  K.<sup>18,19</sup> However, from model fits to the data, deviations from classical behaviour of the soft mode frequency attributed to the onset of quantum fluctuations start to occur at  $\sim 113$  K<sup>18</sup> or  $\sim 155$  K.<sup>19</sup> Katsufuji and Takagi<sup>14</sup> obtained 162 K from similar fitting of the temperature dependence of the dielectric constant. Such fluctuations would need to couple with the acoustic modes to give the observed softening. Spalek<sup>29</sup> observed a loss peak in dielectric spectroscopy data at  $\sim 85$ ,  $\sim 105$  and  $\sim 135$  K when measured at 1, 10 and 100 kHz, respectively, which may or may not be related. Elastic softening and acoustic loss suggestive of an additional instability is also seen in  $\text{LaAlO}_3$  at low temperatures.<sup>58</sup>

The final anomaly identified by RUS occurs below  $\sim 70$ - $80$  K and is a slight but definite increase in  $Q^{-1}$  accompanied by softening (Fig. 2). By definition this indicates some aspect of the structure or defects coupled to strain which move on a timescale of  $\sim 10^{-6}$  s under the influence of an externally applied stress. The onset of increasing  $Q^{-1}$  values perhaps correlates with a break in slope of  $\chi T$  near 85 K, where  $\chi$  is the magnetic susceptibility, reported by

Caslin et al.<sup>27</sup> to be due to the onset of dynamically correlated ferromagnetic clusters ahead of the antiferromagnetic ordering transition. Acoustic loss due to such clustering would be indicative of magnetoelastic coupling in  $\text{EuTiO}_3$ , with wider implications for coupling between (anti)ferromagnetic, ferroelectric and ferroelastic properties.

## V. CONCLUSIONS

Softening of single crystal elastic constants of  $\text{EuTiO}_3$ , as measured near  $\sim 1$  MHz, is consistent with a classical octahedral tilting transition at  $T_c \approx 284$  K which is closely analogous to the cubic - tetragonal transition of  $\text{SrTiO}_3$  at  $\sim 106$  K. The amount of softening is somewhat larger, but the form is qualitatively the same and can be accounted for by coupling of macroscopic spontaneous strains with the R-point order parameter. There are no changes between  $\sim 284$  and  $\sim 10$  K that would be indicative of further phase transitions with strain/order parameter coupling. The pattern of acoustic loss is quite different from that of  $\text{SrTiO}_3$ , indicating that ferroelastic twin walls in the tetragonal phase remain mobile only in a narrow temperature interval below  $T_c$ . There is evidence of further strain relaxation, in the form of elastic softening below  $\sim 140$  K and an increase in acoustic loss below  $\sim 80$  K. The mechanism for these is not known but might be related to some influence of the incipient ferroelectric phase transition and the development of magnetically ordered clusters, respectively. If each of the tilting, magnetic and dielectric properties of  $\text{EuTiO}_3$  couple with strain, whether on a long range or purely local scale, it is inevitable that they will also be coupled with each other and, hence, that they can all be tuned by the imposition of external electric, magnetic and strain fields.

## ACKNOWLEDGEMENTS

RUS facilities were established in Cambridge through a grant from the Natural

Environment Research Council of Great Britain to MAC, which is gratefully acknowledged (NE/B505738/1). LJS acknowledges the support of the National Science Centre (NCN) through Grant MAESTRO No. DEC-2012/04/A/ST3/00342. CP acknowledges Financial support in Greece through grants EURYI and MEXT-CT-2006-039047 grants, and in Singapore through Award No. NRF-CRP-4-2008-04 of the Competitive Research Programme. S.S.S. thanks Jesus College, Cambridge, KAZTOMPROM and CHT, Tashkent, for support.

## References

- <sup>1</sup>R. A. Cowley, *Phil. Trans. R. Soc. Lond. A* **354**, 2799 (1996).
- <sup>2</sup>K. A. Müller, and H. Burkard, *Phys. Rev. B* **19**, 3593 (1979).
- <sup>3</sup>K. A. Müller, W. Berlinger, and E. Tosatti, *Z. Phys. B* **84**, 277 (1991).
- <sup>4</sup>B. Hehlen, Z. Kallassy, and E. Courtens, *Ferroelectrics* **183**, 265 (1996).
- <sup>5</sup>J. F. Scott, and H. Ledbetter, *Z. Phys. B* **104**, 635 (1997).
- <sup>6</sup>D. E. Grupp, and A. M. Goldman, *Science* **276**, 392 (1997).
- <sup>7</sup>W. Schranz, P. Sondergeld, A. V. Kityk, and E. K. H. Salje, *Phase Trans.* **69**, 61 (1999).
- <sup>8</sup>A. V. Kityk, W. Schranz, P. Sondergeld, D. Havlik, E. K. H. Salje, and J. F. Scott, *Phys. Rev. B* **61**, 946 (2000).
- <sup>9</sup>A. V. Kityk, W. Schranz, P. Sondergeld, D. Havlik, E. K. H. Salje, and J. F. Scott, *Europhys. Lett.* **50**, 41 (2000).
- <sup>10</sup>L. Arzel, B. Hehlen, F. Dénoyer, R. Currat, K. –D. Liss, and E. Courtens, *Europhys. Lett.* **61**, 653 (2003).
- <sup>11</sup>L. Arzel, B. Hehlen, A. K. Tagantsev, F. Dénoyer, K. D. Liss, R. Currat, and E. Courtens, *Ferroelectrics* **267**, 317 (2002).
- <sup>12</sup>J. F. Scott, E. K. H. Salje, and M. A. Carpenter, *Phys. Rev. Lett.* **109**, 187601 (2012).



- <sup>13</sup>T. Katsufuji, and Y. Tokura, *Phys. Rev. B* **60**, R15021 (1999).
- <sup>14</sup>T. Katsufuji, and H. Takagi, *Phys. Rev.* **64**, 054415, (2001).
- <sup>15</sup>A. Bussmann-Holder, J. Köhler, R. K. Kremer, and J. M. Law, *Phys. Rev. B* **83**, 212102 (2011).
- <sup>16</sup>J. L. Bettis, M.-H. Whangbo, J. Köhler, A. Bussmann-Holder, and A. R. Bishop, *Phys. Rev. B* **84**, 184114 (2011).
- <sup>17</sup>D. S. Ellis, H. Uchiyama, S. Tsutsui, K. Sugimoto, K. Kato, D. Ishikawa, and A. Q R. Baron, *Phys. Rev. B* **86**, 220301 (2012).
- <sup>18</sup>S. Kamba, D. Nuzhnyy, P. Vanek, M. Savinov, K. Knizek, Z. Shen, E. Santava, K. Maca, M. Sadowski, and J. Petzelt, *Eurphys. Lett.* **80**, 27002 (2007).
- <sup>19</sup>V. Goian, S. Kamba, J. Hlinka, P. Vanek, A. A. Belik, T. Kolodiaznyy, and J. Petzelt, *Eur. Phys. J. B* **71**, 429 (2009).
- <sup>20</sup>A. Bussmann-Holder, Z. Guguchia, J. Köhler, H. Keller, A. Shengelaya, and A. R. Bishop, *New J. Phys.* **14**, 093013 (2012).
- <sup>21</sup>J. Köhler, R. Dinnebier, and A. Bussmann-Holder, *Phase Trans.* **85**, 949 (2012).
- <sup>22</sup>M. Allieta, M. Scavini, L. J. Spalek, V. Scagnoli, H. C. Walker, C. Panagopoulos, S. S. Saxena, T. Katsufuji, and C. Mazzoli, *Phys. Rev. B* **85**, 184107 (2012).
- <sup>23</sup>V. Goian, S. Kamba, O. Pacherová, J. Drahokoupil, L. Palatinus, M. Dusek, J. Rohlicek, M. Savinov, F. Laufek, W. Shranz, A. Fuith, M. Kachlik, K. Maca, A. Shkabko, L. Sagarna, A. Weidenkaff, and A. A. Belik, *Phys. Rev. B* **86**, 054112 (2012).
- <sup>24</sup>A. P. Petrovic, Y. Kato, S. S. Sunku, T. Ito, P. Sengupta, L. Spalek, M. Shimuta, T. Katsufuji, C. D. Batista, S. S. Saxena, and C. Panagopoulos, *Phys. Rev. B* **87**, 064103 (2013).
- <sup>25</sup>J.-W. Kim, P. Thompson, S. Brown, P. S. Normile, J. A. Schlueter, A. Shkabko, A. Weidenkaff, and P. J. Ryan, *Phys. Rev. Lett.* **110**, 027201 (2013).

- <sup>26</sup>D. Bessas, K. Z. Rushchanskii, M. Kachlik, S. Disch, O. Gourdon, J. Bednarcik, K. Maca, I. Sergueev, S. Kamba, M. Lezaic, and R. P. Hermann, *Phys. Rev. B* **88**, 144308 (2013).
- <sup>27</sup>K. Caslin, R. K. Kremer, Z. Guguchia, H. Keller, J. Köhler, and A. Bussmann-Holder, *J. Phys.: Condens. Matter* **26**, 022202 (2014).
- <sup>28</sup>V. Scagnoli, M. Allietta, H. Walker, M. Scavini, T. Katsufuji, L. Sagarna, O. Zaharko, and C. Mazzoli, *Phys. Rev. B* **86**, 094432 (2012).
- <sup>29</sup>L. J. Spalek, *Emergent phenomena near selected phase transitions*, Ph. D. thesis, University of Cambridge (2013).
- <sup>30</sup>S. J. Gong, and Q. Jiang, *Phys. Stat. Sol. (b)* **241**, 3033 (2004).
- <sup>31</sup>H. Wu, and W. Z. Shen, *Sol. St. Comm.* **133**, 487 (2005).
- <sup>32</sup>Z. Guguchia, H. Keller, J. Köhler, and A. Bussmann-Holder, *J. Phys: Condens. Matter* **24**, 492201 (2012).
- <sup>33</sup>C. J. Fennie, and K. M. Rabe, *Phys. Rev. Lett.* **97**, 267602 (2006).
- <sup>34</sup>J. H. Lee, L. Fang, E. Vlahos, X. Ke, Y. W. Jung, L. F. Kourkoutis, J.-W. Kim, P. J. Ryan, T. Heeg, M. Roeckerath, V. Goian, M. Bernhagen, R. Uecker, P. C. Hammel, K. M. Rabe, S. Kamba, J. Schubert, J. W. Freeland, D. A Muller, C. J. Fennie, P. Schiffer, V. Gopalan, E. Johnston-Halperin, and D. G. Schlom, *Nature* **466**, 954 (2010).
- <sup>35</sup>Y. Yang, W. Ren, D. Wang, and L. Bellaiche, *Phys. Rev. Lett.* **109**, 267602 (2012).
- <sup>36</sup>M. A. Carpenter, *Am. Mineral.* **92**, 309 (2007).
- <sup>37</sup>D. S. Ellis, H. Uchiyama, K. Sugimoto, K. Kato, and A. Q. R. Baron, *Ferroelectrics* **441**, 42 (2012).
- <sup>38</sup>Z. Guguchia, A. Shengelaya, H. Keller, J. Köhler, and A. Bussmann-Holder, *Phys. Rev. B* **85**, 134113 (2012).

- <sup>39</sup>A. Migliori, and J. L. Sarrao, *Resonant Ultrasound Spectroscopy: Applications to Physics, Materials Measurements and Nondestructive Evaluation* (Wiley, New York, 1997).
- <sup>40</sup>R. E. A. McKnight, M. A. Carpenter, T. W. Darling, A. Buckley, and P. A. Taylor, *Am. Mineral.* **92**, 1665 (2007).
- <sup>41</sup>R. E. A. McKnight, C. J. Howard, and M. A. Carpenter, *J. Phys.: Condens. Matter* **21**, 015901 (2009).
- <sup>42</sup>M. A. Carpenter, A. Buckley, P. A. Taylor, and T. W. Darling, *J. Phys.: Condens. Matter* **22**, 035405 (2010).
- <sup>43</sup>M. A. Carpenter, E. K. H. Salje, and C. J. Howard, *Phys. Rev. B* **85**, 224430 (2012).
- <sup>44</sup>K. A. Müller, and W. Berlinger, *Phys. Rev. Lett.* **26**, 13 (1971).
- <sup>45</sup>S. A. Hayward, and E. K. H. Salje, *Phase Trans.* **68**, 501 (1999).
- <sup>46</sup>A. Migliori, J. L. Sarrao, W. M. Visscher, T. M. Bell, M. Lei, Z. Fisk, and R. G. Leisure, *Physica B* **183**, 1 (1993).
- <sup>47</sup>R. J. Harrison, and S. A. T. Redfern, *Phys. Earth Planet. Inter.* **134**, 253 (2002).
- <sup>48</sup>R. J. Harrison, S. A. T. Redfern, and E. K. H. Salje, *Phys. Rev. B* **69**, 144101 (2004).
- <sup>49</sup>R. J. Harrison, S. A. T. Redfern, A. Buckley and E. K. H. Salje, *J. Appl. Phys.* **95**, 1706 (2004).
- <sup>50</sup>S. Wenyuan, S. Huimin, W. Yening, and L. Baosheng, *J. Physique Coll.* **46**, C10 (1985).
- <sup>51</sup>W. Yening, S. Wenyuan, C. Xiaohua, S. Huimin, and L. Baosheng, *Phys. Stat. Sol. a* **102**, 279 (1987).
- <sup>52</sup>E. K. H. Salje, *Phase trans in ferroelastic and coelastic crystals* (Cambridge University Press, Cambridge, 1990).
- <sup>53</sup>J. Chrosch, and E. K. H. Salje, *J. Appl. Phys.* **85**, 722 (1999).
- <sup>54</sup>W. Lee, E. K. H. Salje, and U. Bismayer, *Phys. Rev. B* **72**, 104116 (2005).

- <sup>55</sup>W. T. Lee, E. K. H. Salje, L. Goncalves-Ferreira, M. Daraktchiev, and U. Bismayer, *Phys. Rev. B* **73**, 214110 (2006).
- <sup>56</sup>M. A. Carpenter, and Z. Zhang, *Geophys. J. Int.* **186**, 279 (2011).
- <sup>57</sup>E. K. H. Salje, X. Ding, Z. Zhao, T. Lookman, and A. Saxena, *Phys. Rev. B* **83**, 104109 (2011).
- <sup>58</sup>M. A. Carpenter, A. Buckley, P. A. Taylor, R. E. A. McKnight, and T. W. Darling, *J. Phys.: Condens. Matter* **22**, 035406 (2010).